Coherent Transistor

Anatoly A. Grinberg and Serge Luryi, *Fellow, IEEE*

***Abstract*—We consider the high-frequency operation of an abrupt-heterojunction transistor with ballistic transport in the base. The *coherent* regime arises at temperatures low enough compared to the injection energy, that the injected minority carriers form a nearly collimated and monoenergetic beam. The coherent transistor can have both the current gain and the power gain at frequencies far above the conventional cutoff. The extended frequency of an intrinsic transistor is limited by the *dispersion* in the minority-carrier times of flight across the base, rather than the average time of flight itself. The unilateral gain U calculated for an exemplary heterostructure, including the parasitics, demonstrates an active behavior of the coherent transistor in extended frequency ranges.**

I. Introduction

IN A RECENT PAPER [1] we discussed the nature of a high-frequency current gain rolloff in heterostructure bipolar transistors (HBT) with collisionless (ballistic) propagation of minority carriers across the base. In an ideal ballistic transistor, the current gain β decreases with increasing frequency entirely because of the dispersion in the velocities and the incident angles of injected electrons. Members of a minority-carrier ensemble, injected into the base at the same time, arrive at the base–collector junction at different times. The variance $\Delta\tau$ in base transit times τ_B has the effect of washing out a modulation of the injection current density introduced at the base–emitter junction by the input signal. The mechanism of current gain degradation in a ballistic transistor is quite similar to the Landau damping of density waves in collisionless plasmas.

The purpose of this work is to discuss the operation of a ballistic transistor, when

$$\Delta\tau \ll \tau_B \tag{1}$$

i.e., when the injected electrons form a *collimated and monochromatic beam.* A good approximation to such a beam results from the passage of electrons across an abrupt heterointerface. For electrons traveling across the base with a normal velocity v_B, a periodic modulation of the injection at the emitter interface with a frequency f sets up an electron density wave of wavelength $\lambda = v_B/f$. When (1) is fulfilled, the amplitude of this wave does not appreciably decay over the entire base width W_B. In this case, we shall be speaking of a "*coherent*" base propagation; transistor operating in such a regime will be referred to as the coherent transistor (CT). It will be shown that the CT can have both the common-emitter current gain β and the power gain exceeding unity at frequencies far above the usual f_T, limited by the base propagation time.

It should be clear from the outset that the coherent operation is likely to require cryogenic temperatures. The band structure of an HBT can be engineered [2] in such a way that the minority carriers are injected into the base "over a cliff" (Fig. 1) of energy Δ; we shall refer to this type of transistor as the abrupt-junction HBT or a-HBT. For the ballistic regime of minority transport to hold over the entire base width (and we shall be interested in rather long bases, $W_g \gtrsim 1000$ Å), the injection energy should be arranged so as not to exceed the optical phonon emission threshold $\Delta \lesssim \hbar\omega_{\rm opt}$. Typical values of $\hbar\omega_{\rm opt}$ are 54 meV in Si and 36 meV in GaAs. To fulfill (1), on the other hand, the electron kinetic energy Δ must substantially exceed the thermal spread, whence we need

$$\hbar\omega_{\rm opt} \gtrsim \Delta = \frac{mv_B^2}{2} \gg kT \tag{2}$$

which means that the implementation of a CT requires at least liquid N_2 temperatures.

The possibility of using transit-time phase shifts in a bipolar junction transistor to extend the active transistor operation into a range of frequencies beyond the usual f_T has been discussed by a number of researchers [3]–[8]. A cornerstone of that discussion has been the negative dynamic output impedance, which can be achieved due to the phase delay in minority-carrier drift across the collector space-charge region, as proposed originally by Wright [3]. This idea, attractive for millimeter- and submillimeter-wave applications, has gained a lot of attention [4]–[10]. Besides further developing Wright's "translator" concept, assuming [4], [5] a conventional junction transistor implementation, several authors considered similar concepts in the context of HBT [6]–[8], unipolar ballistic transistors [9], and field-effect transistors [10].

Transistor transit-time oscillators can be regarded [3]–[5] as a dipole between emitter and collector, with the base being open-circuited at RF while normally biased in dc. From this point of view, the "translator" is quite similar to transit-time diodes [11]. The negative dynamic resistance arises from a combination of the injection phase delay $\varphi = \varphi_E + \varphi_B$ (the total transit angle of the emitter and the base) and the drift delay θ in the base–collector junction.

Manuscript received December 4, 1992; revised April 12, 1993. The review of this paper was arranged by Associate Editor N. Moll.

The authors are with AT&T Bell Laboratories, Murray Hill, NJ 07974.

IEEE Log Number 9209863.

0018-9383/93$03.00 © 1993 IEEE

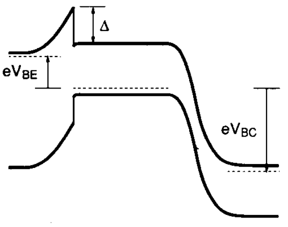

Fig. 1. Schematic band diagram of an abrupt-junction heterostructure bipolar transistor (a-HBT). Minority carriers are injected into the base "over a cliff" of energy Δ.

A more general point of view [6]-[10] is to consider the negative-resistance frequency regions as resonances in the unilateral power gain U, which is defined [12] as the maximum available power gain of a device after it has been made unilateral by adding a lossless reciprocal feedback circuit. Realization of a maximum available gain requires the load resistance be matched to the output resistance Re (z_{22}). If the latter is negative, then the gain can be increased [9] by including an additional positive resistance in series with z_{22}. It is, therefore, possible, in principle, to use transistors with a negative output resistance for the implementation of high-gain amplifiers as well as oscillators.[1]

Unfortunately, however, the practical possibility of extending the active transistor behavior beyond f_T is severely limited by parasitic effects. According to Tiwari [8], the utilization of transit-time resonances, arising from carrier drift across the collector junction in a conventional GaAs/AlGaAs HBT with diffusive base transport, requires a reduction of the base and collector resistances, as well as the collector capacitance, by factors of 10 from estimates, based on the state-of-the-art technology.

As will be shown in the present work, there is a twofold reason why the transit-time effects in conventional bipolar transistors are swamped by the device parasitics. On the one hand, the exponential decay of the base transport factor $|\alpha_0| \sim e^{-\varphi_B}$ with the phase φ_B acquired in a diffusive propagation of minority carriers across the base, implies that the overall phase of the collector current $(\varphi_B + \varphi_E + \theta)$ must be acquired almost entirely at the expense of the collector phase delay θ. On the other hand, the increasing θ also diminishes the negative dynamic resistance of an intrinsic transistor below the level necessary to overcome the influence of parasitic elements. Collisionless base propagation by itself does not qualitatively change this situation, because of the Landau damping of the current gain [1]. Only in the coherent regime, (1), is it possible to acquire a sufficient phase $\varphi_B \gtrsim \pi$ in the base transport alone without a significant penalty in the magnitude of the base transport factor α_B.

The current gain of a coherent transistor is discussed in the next section. It will be shown there that an ideal CT (without external resistances or capacitances and neglecting a transit delay θ in the base-collector junction) has $\beta > 1$ in a set of resonant bands of frequencies centered at $f_\nu = 2\pi\nu f_T$, $\nu = 1, 2, \cdots$, where $f_T = (2\pi\tau_B)^{-1}$ is the usual cutoff frequency of such a transistor. Including the collector delay θ, we shall show that *increasing the base width*, and therefore the delay φ_B, can lead to a strong enhancement of β in the frequency range where for $\varphi_B = 0$ one had $\beta << 1$. A simple physical picture of this effect will be presented.

It will be also shown in Section II that magnitudes of the resonant peaks themselves decrease with the frequency as $\beta(f_\nu) = 1/(2\pi^2 f_\nu^2 \Delta\tau_B^2)$, where $\Delta\tau_B^2 \equiv \langle\tau_B^2\rangle - \langle\tau_B\rangle^2$. This means that in a coherent base propagation by minority carriers it is the dispersion in their time of flight, rather than the average time of flight itself, that determines the extended current gain cutoff frequency f_x. Under the condition (1), the fundamental cutoff f_x can substantially exceed f_T.

The unilateral gain of a coherent transistor will be considered in Section III. Our analysis will be based on an equivalent circuit [8] that includes both the internal parameters and the external parasitic elements. It will be shown that the coherent base propagation can change the transistor behavior from passive to active. We find that the CT has an active behavior in extended frequency bands even when we include realistic values of the base and collector resistance.

To facilitate the search for optimum parameters, we derived analytic expressions for U, z_{22}^e, and h_{21}^e in an explicit form that includes the parasitics and can be applied to heterojunction as well as homojunction transistors both in the ballistic and the diffusion regimes. This helps to identify the parameters that must be minimized in a practical realization of the coherent transistor. An exemplary CT structure is discussed in Section IV and our conclusions are summarized in Section V.

II. CURRENT GAIN

Consider first the base transport factor α_B for a "perfectly" coherent transistor, in which all injected electrons travel toward the collector with the same velocity $v_B = (2\Delta/m)^{1/2}$. In this case, a periodic modulation of the injection at the emitter interface sets up in the base an electron density wave of the form

$$n(z, t) = n_0 e^{i\omega(t - z/v_B)} \tag{3}$$

where n_0 is the amplitude of the concentration modulation. At any point in the base, the electron current density $J(z, t)$ equals $-env_B$ and the complex transport factor α_B hence is

$$\alpha_B \equiv \frac{J(W_B, t)}{J(0, t)} = e^{-i\omega\tau_B} \tag{4}$$

---

[1] We remark that power gain in the translator frequency bands, where Re $(z_{22}) < 0$, is not accompanied by a common emitter current gain β exceeding unity. The narrow-band figure of merit $f_{\max}$ of such devices substantially exceeds their broad-band figure f_T. As will be shown in Section 2, the coherent mode of base propagation modifies the usual 10-dB/decade rolloff in β and opens up ranges of frequency, where $\beta > 1$, above the conventional f_T. This effectively makes f_T a narrow-band figure of merit in the CT.

where $\tau_B \equiv W_B/v_B$. In an intrinsic transistor, the common-emitter current gain is given by $\alpha_B/(1 - \alpha_B)$ and equals

$$h_{21}^e = \frac{\exp(-i\omega\tau_B/2)}{2i \sin(\omega\tau_B/2)} \tag{5a}$$

$$\beta \equiv |h_{21}^e| = \frac{1}{2|\sin(\omega\tau_B/2)|} \underset{\omega\tau_B < 1}{\approx} \frac{1}{\omega\tau_B}. \tag{5b}$$

The usual procedure for the determination of f_T in a microwave transistor is to extrapolate the data measured at relatively low frequencies to unity gain at 20 dB/decade. Since for $\omega\tau_B \lesssim 1$ the current gain of a CT rolls off very accurately as ω^{-1} (i.e., 20 dB/decade), as seen from (5b), the extrapolation procedure will produce the usual value

$$f_T = \frac{1}{2\pi\tau_B}. \tag{6}$$

However, in a coherent transistor f_T is not the fundamental current gain cutoff. Equation (5b) indicates the existence of frequency windows, centered at $f_\nu = 2\pi\nu f_T$, or

$$\omega_\nu \tau_B = 2\pi\nu, \qquad \nu = 1, 2, \cdots \tag{7}$$

and characterized by $\beta > 1$. The physical origin of this effect is evident from Fig. 2. Neglecting recombination in the base, the only reason that the base current is flowing in a microwave transistor is to maintain neutrality of the base layer by screening the injected charge. The resonant frequencies f_ν correspond to an integer number ν of periods $\lambda = v_B/f$ of the density wave (3) in the base. To the extent that the wave is not decaying in amplitude in a perfect CT, the total minority-carrier charge in resonance does not fluctuate at all. The output current modulation is thus accomplished with no RF current input, hence the "infinite" gain.

Note that in a diffusion transistor, the minority-carrier concentration amplitude must necessarily decay with the distance toward the collector and hence the total injected charge in the base oscillates at any frequency. A similar effect occurs in an incoherent ballistic transistor, due to the Landau damping of minority-carrier density waves. In an imperfectly coherent transistor, the density wave is Landau damped to some extent and the base current has a finite value at all frequencies. This idea is mathematically expressed as follows.

Consider the intrinsic current gain of the ballistic a-HBT, taking into account a realistic inbound electron distribution at the base-emitter interface. For a thermal distribution the result is given by [1, eq. (14)]. In the limit of slow recombination, $\tau_{cp} \gg \tau_B$, where τ_{cp} is the capture time for electrons at energy Δ, that equation reduces to

$$\alpha_B = \int_0^\infty e^{-\epsilon - i\omega\tau(\epsilon)}\, d\epsilon \tag{8}$$

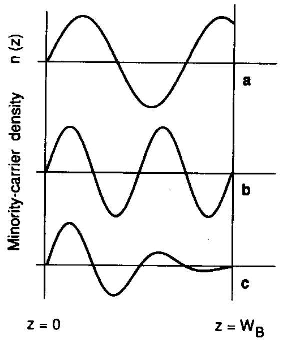

Fig. 2. Minority-carrier density wave, propagating with a speed v_B across the base of a ballistic transistor. The wavelength λ_B equals $2\pi v_B/\omega$. Resonances in β arise when $W_B = \nu\lambda_B$. *a*: coherent, off-resonance; *b*: coherent, in resonance; *c*: Landau damped.

where

$$\tau(\epsilon) \equiv \frac{\tau_T}{(\tilde{\Delta} + \epsilon)^{1/2}} \qquad \tilde{\Delta} \equiv \frac{\Delta}{kT}$$
$$\tau_T \equiv \frac{W_B}{v_T} \qquad v_T \equiv \left(\frac{2kT}{m}\right)^{1/2}. \tag{9}$$

The frequency dependence of $\beta = |\alpha_B/(1 - \alpha_B)|$, calculated from (8), is shown in Fig. 3, where we plot $\beta^2(\omega)$ assuming the dimensionless coherence parameter $\tilde{\Delta} = 5$ and the values of Δ and W_B such that $\tau_B = 1$ ps. The gain peaks occur approximately at f_ν given by (7), their magnitude decreasing with the frequency as f_ν^{-2}.

In the CT limit $\tilde{\Delta} \gg 1$, we find from (8) the following asymptotic expression for α_B:

$$\alpha_B = \frac{e^{-i\omega\tau_B}}{1 - i\omega\tau_B/2\tilde{\Delta}}. \tag{10}$$

The approximate dependence $\beta^2(\omega)$, calculated from (10) is plotted in Fig. 3 by the dotted line. We see that (10) gives an excellent approximation to the exact result (8) for $\tilde{\Delta} = 5$. It can be used, therefore, to calculate the peak gain values. The maxima β_ν occur at those values of $\omega = \omega_\nu$ where Im $(\alpha_B) = 0$ while Re $(\alpha_B) > 0$. Whence we find

$$\beta_\nu = \frac{8\tilde{\Delta}^2}{(\omega_\nu\tau_B)^2} \approx \frac{2\Delta^2}{(\nu\pi kT)^2} \tag{11}$$

which shows that the peaks are proportional to $\tilde{\Delta}^2$ and decrease with the frequency as ω^{-2}.

It is instructive to derive the result (11) in a different fashion, allowing for more general—not necessarily thermal—incident electron distributions at the base-emitter interface. We can interpret (8) as an average $\langle \exp(-i\omega\tau) \rangle$ over a distribution of the times of flight τ, viz.

$$\alpha_B = \int \rho(\tau) e^{-i\omega\tau}\, d\tau. \tag{12}$$

In other words, α_B represents the characteristic function [14] of a random variable τ. Suppose that τ is distributed

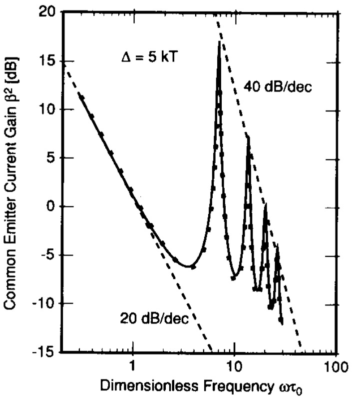

Fig. 3. The intrinsic common-emitter current gain of a coherent transistor. Solid line shows $\beta^2(\omega) \equiv |h^e_{21}|^2$, calculated from (9), dotted line from (11). The dashed lines indicate the gain rolloff in the conventional frequency range ($f < f_T$) and the extended range ($f > f_T$).

normally with a mean $\bar{\tau}$ and a dispersion $\Delta\tau$

$$\rho(\tau) \propto e^{-(\tau-\bar{\tau})^2/2\Delta\tau^2}. \tag{13}$$

The characteristic function of this distribution is [14]

$$\alpha_B = e^{-i\omega\bar{\tau}} e^{-(\omega\Delta\tau)^2/2}. \tag{14}$$

The maxima of $\beta(\omega) = |\alpha_B/(1 - \alpha_B)|$, with $\alpha_B(\omega)$ given by (14), occur at $\omega = \omega_\nu$, where

$$\omega_\nu \bar{\tau} = 2\pi\nu, \qquad \nu = 1, 2, \cdots \tag{15}$$

and for $\omega\Delta\tau \lesssim 1$ they are given by

$$\beta(\omega_\nu) \approx \frac{2}{\omega_\nu^2 \Delta\tau^2}. \tag{16}$$

The thermal distribution (8) corresponds to $\rho(\tau) = \exp(\tau_T^2/\tau^2 - \tilde{\Delta})$, as seen by substituting $\epsilon(\tau) = (\tau_T/\tau)^2 - \tilde{\Delta}$ [from (9)] into $\rho(\tau) = \exp[-\epsilon(\tau)]$. For this distribution, we find to lowest order in $\tilde{\Delta}^{-1}$.

$$\bar{\tau} = \tau_B, \qquad \Delta\tau^2 \equiv \langle(\tau - \bar{\tau})^2\rangle \approx \frac{\tau_T^2}{4\tilde{\Delta}^3} = \left(\frac{\bar{\tau}}{2\tilde{\Delta}}\right)^2 \tag{17}$$

which shows that (16) is in agreement with (11). Equation (16) demonstrates that for a coherent base propagation of minority carriers, the fundamental current gain cutoff is determined by the dispersion in their times of flight $f_x \approx 1/(\sqrt{2}\,\pi\Delta\tau)$.

In contrast, for a diffusive minority-carrier base propagation the high-frequency complex transport factor is of the form

$$\alpha_B = \frac{1}{\cosh[(2i\omega\tau_D)^{1/2}]} \approx \begin{cases} (1 + i\omega\tau_D)^{-1}, & \text{for } \omega\tau_D \ll 1 \\ 2e^{-\omega\tau_D} e^{-i\omega\tau_D}, & \text{for } \omega\tau_D \gtrsim 1 \end{cases} \tag{18}$$

where $\tau_D = W_B/2D$ is the base transit time by diffusion. Accordingly, the current gain at low frequencies equals $\beta = 1/\omega\tau_D$ and rolls off at 20 dB/dec, but above f_T the gain becomes exponentially small. The phase shift of order 2π is reached only when $|\alpha_B|$ has become small and there is no room for useful resonances. For the same reason, the base transit angle φ_B cannot be optimized in a transistor based on diffusive transport. The total injection delay $\varphi = \varphi_B + \varphi_E$ in Wright's translator is mainly due to a capacitive phaseshift φ_E, like in BARITT oscillators, and is far from reaching the optimum value $\varphi = \pi$ featured by IMPATT diodes [11].

The stark contrast between the coherent ballistic and the diffusive modes of base transit by minority carriers, can also be seen from Fig. 4, where we include a transit angle $\theta \equiv \omega\tau_C$ across the base–collector junction. As is well known, the inclusion of θ in the overall common-base gain h^b_{21} is accomplished by multiplying α_B with a collector transport factor α_C, i.e.,

$$h^e_{21} = \frac{\alpha_B \alpha_C}{1 - \alpha_B \alpha_C}. \tag{19}$$

Assuming a saturated drift velocity v_s, one has [13]

$$\alpha_C = \frac{1 - e^{-i\theta}}{i\theta} = \frac{\sin(\theta')\, e^{-i\theta'}}{\theta'} \tag{20}$$

where $\theta' = \omega\tau'_C$ and $\tau_C = 2\tau'_C = W_C/v_s$ with W_C being the width of the base–collector space-charge layer. The dotted line in Fig. 4(a) shows the common-emitter current gain, limited only by the collector transit $\tau_C = 1$ ps. This curve corresponds to setting $\tau_D = \tau_B = 0$, which gives $\alpha_B = 1$ for either diffusive or ballistic base transport. The dashed line corresponds to a diffusive transport with $\tau_D = 2$ ps (while keeping the same $\tau_C = 1$ ps). The cutoff has shifted to lower frequencies, as expected. The solid line represents a ballistic transistor with $\tau_C = 1$ ps, $\tau_B = 2$ ps, and $\tilde{\Delta} = 10$. We see the dramatic re-emergence of a large gain in the frequency range, where not only the diffusive transistor, *but even the transistor with no base delay at all*, are completely damped. The origin of this effect is evident from Fig. 4(b), where, following [1], we plot the complex trajectories $\alpha(f) = -h^b_{21}$ for the same three cases as in Fig. 4(a). Solid circles mark the positions, corresponding to the peak frequency f_p in Fig. 4(a). We see that the addition of a coherent delay boosts the overall phase of α by the amount $\varphi_B \approx 2\pi(1 - f_p\tau'_C)$, bringing about the condition [Im $(\alpha) \approx 0$, Re $(\alpha) > 0$] that maximizes β, while $|\alpha|$ is still large (≈ 0.7).

It is instructive to consider the following question: why is it that the phase shift, obtained in a coherent base transport, is advantageous compared to that arising in the saturated-velocity transport across the base–collector space-charge region? After all, both delays are gained in a constant velocity carrier propagation. We have not even considered the dispersion in the transit angle θ, arising from the distribution of hot-carrier velocities in the collector junction, which would further degrade all transit-time effects, arising from the transport across that junction. Mathematically, the answer is evident from (19) and (20): the disadvantage of a saturated-velocity propagation results from the factor $\sin(\theta')/\theta'$ which diminishes the magnitude of the complex transport factor α_C at high frequencies. Physically, the difference is rooted in the *nature*

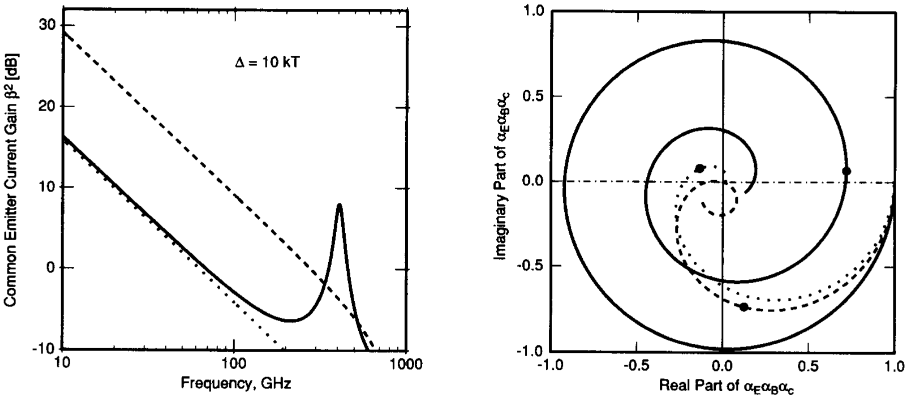

(a) (b)

Fig. 4. The intrinsic current gain, including the collector delay $\tau_C = 1$ ps. Dashed lines correspond to zero base delay, dotted lines to a diffusive delay $\tau_D = 2$ ps, and solid lines to a CT with $\tilde{\Delta} = 10$ and a ballistic delay $\tau_B = 2$ ps. (a) $\beta^2 \equiv |h_{21}^2|^2$ versus frequency. (b) Phase trajectories of $\alpha(\omega) \equiv -h_{21}^b$. Solid circles mark the positions corresponding to the peak frequency $f_P \approx$ 400 GHz of the solid curve in part (a).

of screening of a dynamic charge moving *inside* or *outside* a conductor. Minority carriers moving inside the base induce a base current only to the extent that their total charge varies in time. Under the condition (7), the base RF current vanishes, while the collector current (neglecting θ) oscillates in phase with the minority-carrier density arriving at the junction. In contrast, carriers moving in the depleted layer induce currents of equal magnitude in both the base and the collector electrodes [15].

III. THE UNILATERAL GAIN, INCLUDING TRANSIT-TIME EFFECTS

Fig. 5 shows an equivalent circuit of a ballistic HBT with abrupt emitter–base heterojunction. It includes the intrinsic parameters R_E and C_E (the differential resistance and capacitance of the emitter–base junction, respectively), C_C (the collector junction capacitance $\alpha = \alpha_E\alpha_B\alpha_C$ (product of the emitter, base, and collector transport factors), and R_B (the intrinsic base resistance), as well as the extrinsic collector capacitance C_{Cx} and the parasitic resistances R_{Bx}, R_{Cx}, and R_{Ex}. We are interested in calculating the unilateral gain U of this model two-port, assuming an abrupt-junction HBT with ballistic base propagation. For comparison, we shall also consider the case of a-HBT with diffusive base transport. We shall refer to these two models as the a-HBT(B) and the a-HBT(D), respectively. The coherent transistor is evidently a special case of a-HBT(B)—supplemented with condition (2).

Neglecting R_B, the common-base intrinsic admittance parameters are given by

$$Y^{bi}[\text{a-HBT(D)}] = \begin{pmatrix} g_E + i\omega C_E & 0 \\ -g_E\alpha_B\alpha_C & \dfrac{g_A\alpha_C\lambda W_B \tanh(\lambda_D W_B)}{\cosh(\lambda_D W_B)} + i\omega C_C \end{pmatrix} \tag{21a}$$

$$Y^{bi}[\text{a-HBT(B)}] = \begin{pmatrix} g_E + i\omega C_E & 0 \\ -g_E\alpha_B\alpha_C & i\omega C_C \end{pmatrix} \tag{21b}$$

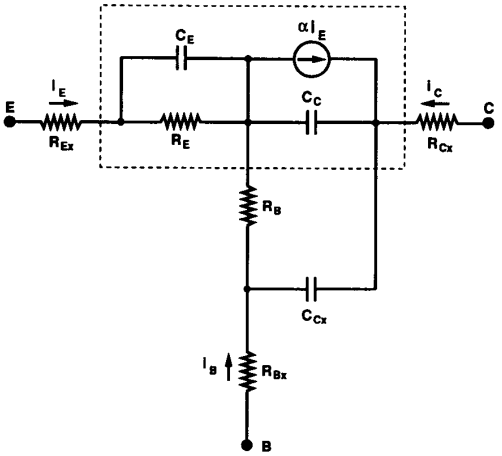

Fig. 5. Equivalent circuit of an abrupt-junction heterostructure bipolar transistor with ballistic propagation of minority carriers. The intrinsic portion, corresponding to the matrix (21b), is indicated by a dashed line. For diffusive transistors, the intrinsic portion must be replaced by a two-port block described by matrices (21a) or (22).

where $g_E \equiv 1/R_E$ is the differential emitter conductance, $g_A \equiv g_E(kT/eV_A)$, with V_A being the Early voltage, $\lambda = \lambda_D(1 + i\omega\tau_{cp})^{1/2}$, and $\lambda_D = (D\tau_{cp})^{-1/2}$ with τ_{cp} being the recombination time of thermalized electrons in the base. The collector transport factor α_C is defined by (20). The two expressions (21) differ by the Early effect, which modulates the output conductance in a-HBT(D), while being entirely absent in a-HBT(B). If the Early effect is neglected, then both expressions are formally identical, but the base transport factors α_B involved are different. For a-HBT(B) the complex α_B is given generally by (8) and in the CT limit (assumed henceforth) by (10), whereas for a-HBT(D) one has $\alpha_B = 1/\cosh(\lambda W_B)$. Portion of the equivalent circuit described by (21b) is shown in Fig. 5 by the dashed line. Note that this circuit does not describe diffusive transistors. To agree with (21a), the indicated portion of the circuit has to be modified in accordance with the Early effect.

The a-HBT(D) model [16], [17] should be carefully distinguished[2] from the case of a graded-gap emitter–base junction (g-HBT), considered previously [8] in the context of transit-time effects on the unilateral gain. Small-signal operation of a diffusive g-HBT is described by the classical bipolar (homo)junction transistor (BJT) theory (cf. [18], [19])

$$Y^{\mathrm{bi}}[\text{g-HBT}] = \begin{bmatrix} \dfrac{g_E \lambda \tanh(\lambda_D W_B)}{\lambda_D \tanh(\lambda W_B)} + i\omega C_E & -\dfrac{g_A \lambda W_B}{\cosh(\lambda_D W_B)\sinh(\lambda W_B)} \\ -\dfrac{g_E \alpha_C \lambda \tanh(\lambda_D W_B)}{\lambda_D \sinh(\lambda W_B)} & \dfrac{g_A \alpha_C \lambda W_B}{\cosh(\lambda_D W_B)\tanh(\lambda W_B)} + i\omega C_C \end{bmatrix}. \tag{22}$$

The unilateral gain U can be calculated from any of the following equivalent expressions:

$$U = \frac{|z_{21} - z_{12}|^2}{4[\mathrm{Re}\,(z_{11})\,\mathrm{Re}\,(z_{22}) - \mathrm{Re}\,(z_{12})\,\mathrm{Re}\,(z_{21})]} \tag{23a}$$

$$= \frac{|y_{21} - y_{12}|^2}{4[\mathrm{Re}\,(y_{11})\,\mathrm{Re}\,(y_{22}) - \mathrm{Re}\,(y_{12})\,\mathrm{Re}\,(y_{21})]} \tag{23b}$$

$$= \frac{|h_{21} + h_{12}|^2}{4[\mathrm{Re}\,(h_{11})\,\mathrm{Re}\,(h_{22}) + \mathrm{Im}\,(h_{12})\,\mathrm{Im}\,(h_{21})]} \tag{23c}$$

where z_{ij}, y_{ij}, and h_{ij} are the impedance, the admittance, and the hybrid parameters of a transistor, respectively. For the case of a-HBT(B) the common-emitter impedance matrix

$$Z^e = \begin{pmatrix} z^e_{11} & z^e_{12} \\ z^e_{21} & z^e_{22} \end{pmatrix} \tag{24}$$

is easily calculated from the equivalent circuit in Fig. 5

$$z^e_{11} = \frac{R_B[(1 - \alpha_E\alpha_B\alpha_C)C_{Cx} + C_C]}{C_{Cx} + C_C(1 + i\omega R_B C_{Cx})} + \alpha_E R_E + R_{Bx} + R_{Ex} \tag{25a}$$

$$z^e_{12} = \frac{(1 - \alpha_E\alpha_B\alpha_C)R_B C_{Cx}}{C_{Cx} + C_C(1 + i\omega R_B C_{Cx})} + \alpha_E R_E + R_{Ex} \tag{25b}$$

$$z^e_{21} = \frac{-\alpha_E\alpha_B\alpha_C(1 + i\omega R_B C_{Cx}) + i\omega R_B C_{Cx}}{i\omega[C_{Cx} + C_C(1 + i\omega R_B C_{Cx})]} + \alpha_E R_E + R_{Ex} \tag{25c}$$

$$z^e_{22} = \frac{(1 - \alpha_E\alpha_B\alpha_C + i\omega R_E C_C \alpha_E)(1 + i\omega R_B C_{Cx}) + i\omega R_E C_{Cx}\alpha_E}{i\omega[C_{Cx} + C_C(1 + i\omega R_B C_{Cx})]} + R_{Ex} + R_{Cx}. \tag{25d}$$

Using (23a) and (25) we obtain for U the following expression:

$$U = \frac{|\alpha_E\alpha_B\alpha_C|^2}{4[\Gamma_3 - \mathrm{Re}\,(\alpha_E\alpha_B\alpha_C)\cdot\Gamma_1 - \mathrm{Im}\,(\alpha_E\alpha_B\alpha_C)\cdot\Gamma_2]} \tag{26}$$

where

$$\Gamma_1 = \omega^2 R_B C_{Cx}(R_{Bx}C_{Cx} + R_{Cx}C_C + R_{Cx}C_{Cx}) \tag{27a}$$

$$\begin{aligned} \Gamma_2 = {} & \omega R_B C_C[1 + (R_{Bx}/R_B)(1 + C_{Cx}/C_C) \\ & + \omega^2 R_B(R_{Bx} + R_{Cx})C^2_{Cx}] \end{aligned} \tag{27b}$$

$$\begin{aligned} \Gamma_3 = {} & |\alpha_E|^2\omega^2 R_E R_B C^2_C(1 + [(R_{Bx} + R_{Cx})/R_B] \\ & \cdot [(1 + C_{Cx}/C_C)^2 + (\omega R_B C_{Cx})^2]) \\ & + \omega^2 C^2_C(R_B[R_{Ex} + R_{Cx}(1 + C_{Cx}/C_C)^2 \\ & + R_{Bx}(C_{Cx}/C_C)^2] \\ & + (R_{Bx}R_{Ex} + R_{Bx}R_{Cx} + R_{Cx}R_{Ex}) \\ & \cdot [(1 + C_{Cx}/C_C)^2 + (\omega R_B C_{Cx})^2]) \end{aligned} \tag{27c}$$

and

$$\alpha_E \equiv \frac{1}{1 + i\omega\tau_E}, \qquad \tau_E \equiv R_E C_E. \tag{27d}$$

---

[2] The two models lead to qualitative differences in the electrical characteristics, both static and high-frequency. The difference is rooted in the fact that while the quasi-Fermi level E_{F_n} of minority carriers is continuous in the g-HBT, like it is in a BJT, in the a-HBT(D), like in a forward-biased Schottky diode, E_{F_n} suffers a discontinuity at the emitter-base interface. Of course, for a ballistic transport of minority carriers the E_{F_n} concept is not applicable at all.

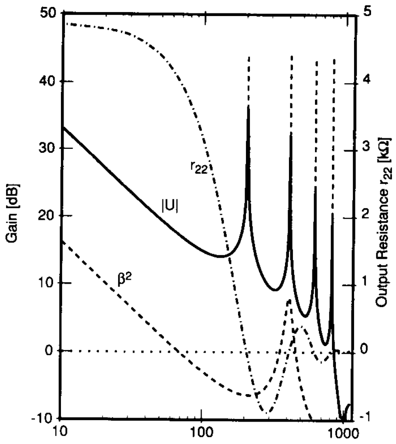

Fig. 6. Frequency dependences of the unilateral gain $|U|$, the output resistance $r_{22} \equiv \text{Re}\,(z^e_{22})$, and the common-emitter current gain $\beta \equiv |h^e_{21}|$ in the intrinsic limit of a coherent transistor. Assumed parameters: $\tilde{\Delta} = 10$, $\tau_C = 1$ ps, $\tau_B = 2$ ps, $C_C = 0.5$ fF, $R_E = 5\ \Omega$, $R_B = 25\ \Omega$.

The current gain $h^e_{21} = -z^e_{21}/z^e_{22}$ is of the form

$$h^e_{21} = \frac{(\alpha_E\alpha_B\alpha_C - i\omega R_E C_C \alpha_E)(1 + i\omega R_B C_{Cx}) - i\omega(R_{Ex}C'_C + R_E C_{Cx}\alpha_E + R_B C_{Cx})}{[(1 - \alpha_E\alpha_B\alpha_C) + i\omega R_E C_C \alpha_E](1 + i\omega R_B C_{Cx}) + i\omega[R_E C_{Cx}\alpha_E + (R_{Ex} + R_{Cx})C'_C]} \tag{28}$$

where $C'_C \equiv C_C + C_{Cx} + i\omega R_B C_C C_{Cx}$. Formulas (24)–(28) are valid for a-HBT(B); they retain the same form for a-HBT(D) if the Early effect is neglected. Similar formulas, neglecting the Early effect, and valid for g-HBT with either diffusive or ballistic transport, as well as general expressions for h^e_{21}, including the Early effect, are presented in the Appendix.

The product of three transport factors in (26) is given by

$$\text{Im}\,(\alpha_E\alpha_B\alpha_C) = \frac{\cos(\varphi + \theta) - \cos(\varphi)}{\theta}\,|\alpha_E\alpha_B| \tag{29a}$$

$$\text{Re}\,(\alpha_E\alpha_B\alpha_C) = \frac{\sin(\varphi + \theta) - \sin(\varphi)}{\theta}\,|\alpha_E\alpha_B| \tag{29b}$$

where $\varphi = \varphi_E + \varphi_B$, $\varphi_E \equiv \omega\tau_E$, $\varphi_B \equiv \omega\tau_B$, and $\theta \equiv \omega\tau_C$.

Consider first the intrinsic limit $R_{Ex} = R_{Bx} = R_{Cx} = 0 = C_{Cx}$. The output impedance, (25d), becomes

$$z^e_{22} = \frac{1 - \alpha_E\alpha_B\alpha_C}{i\omega C_C} + \alpha_E R_E \equiv r_{22} + ix_{22}. \tag{30}$$

If we assume for simplicity that $\omega\tau_E \ll 1$, then $\alpha_E = e^{-i\omega\tau_E}$ to first order in $\omega\tau_E$ and we have

$$r_{22} = \frac{\cos(\varphi) - \cos(\varphi + \theta)}{\omega C_C \theta}\,|\alpha_B| + R_E \tag{30a}$$

$$x_{22} = -\frac{\theta + \sin(\varphi) - \sin(\varphi + \theta)}{\omega C_C \theta}\,|\alpha_B| - R_E\varphi_E \tag{30b}$$

in agreement[3] with [4] and [7]. The unilateral gain assumes the form

$$U = \frac{|\alpha_B\alpha_C|^2}{4\omega R_B C_C}\,\frac{1}{\omega R_E C_C - \text{Im}\,(\alpha_E\alpha_B\alpha_C)} = \frac{|\alpha_B\alpha_C|^2}{4\omega^2 C_C^2 R_B r_{22}}. \tag{31}$$

The frequency dependences of $|U|$, r_{22}, and $|h^e_{21}|^2$ in the intrinsic limit of a CT are plotted in Fig. 6. Note that while in the low-frequency region one has $U > 0$, the sign of U changes on passing the peaks of $|U|$. In the range where $U < 0$, the transistor is active even if $|U| < 1$, since one can bring about the regime with $U > 1$ by adding an external resistance. For positive U, the activity criterion remains the usual $U > 1$. This condition is fulfilled in the entire range between the second and the third peak, where the output resistance is positive. We see that the condition $r_{22} < 0$ is not a necessary requirement for the transistor to be active in an extended frequency range.

Next, consider a model in which we retain the parasitic resistances but eliminate the extrinsic capacitance $C_{Cx} = 0$. In this case, to within terms linear in $\omega\tau_E$, the unilateral gain can be reduced to the following form:

$$U = \frac{|\alpha_B\alpha_C|^2}{4\omega^2 C_C^2 (R_B + R_{Bx})}\,\frac{1}{R_x^{\text{eff}} + r_{22}} \tag{32}$$

---

[3] For BJT transit-time oscillators, Wright's original paper [4] gives a more general result, which includes the Early effect and allows for a nonuniform base doping.

where $R_x^{\text{eff}} = R_{Cx}(R_E + R_{Ex})/(R_B + R_{Bx})$ and

$$r_{22} = \frac{\cos(\varphi) - \cos(\varphi + \theta)}{\omega C_C \theta} |\alpha_B| + R_E + R_{Ex} + R_{Cx}. \tag{33}$$

Equations (32) and (33) show that when parasitic elements are included, then the condition of negative output resistance does not imply $U < 0$ (the converse is still true, U can only be negative if $r_{22} < 0$). These equations demonstrate the root of the discouraging result in Tiwari's analysis [8] of the diffusive transistor. Indeed, with diffusive transport in the base there is no way of avoiding a penalty in the magnitude of the factor (29a) responsible for negative output resistance. In the intrinsic case, this factor has only a mild competition from $\omega C_C R_E$ and the negative dynamic r_{22} can easily be achieved, so long as R_E is sufficiently low. With the parasitic elements added, we need to minimize the resistance $(R_x^{\text{eff}} + r_{22})$, which requires the factor (29a) be large and negative. If $\varphi << 1$ and $\varphi + \theta = 2\pi$, then (29a) equals $-|\alpha_B|\varphi^2/4\pi\omega C_C$, which is small even for $|\alpha_B| \approx 1$. On the other hand, if the condition $\varphi + \theta = 2\pi$ is accomplished with approximately equal contributions from both $\varphi_B \approx \theta \approx \pi$, then, for the diffusive transport mechanism, the factor (29a) becomes small because of $\alpha_B \sim \exp(-\varphi_B)$. With realistic values of the parasitics, this factor is inadequate for making U negative.

With the coherent transport in the base, we have the opportunity to enhance the overall phase by increasing the delay φ_B, keeping the collector delay $\theta \lesssim 1$. In this case, the factor (29a) becomes approximately equal $[-\sin(\varphi + \theta')]$ and for $\varphi + \theta' \approx 3\pi/2$ the output impedance r_{22} is negative, provided

$$\omega C_C(R_E + R_{Ex} + R_{Cx} + R_x^{\text{eff}}) < 1. \tag{34}$$

Note that the longer the base, the lower the frequency at which the phase relation in (29a) is optimal. Therefore, inequality (34) can be fulfilled, provided the base width W_B is sufficiently long, while the base transport can still be regarded as ballistic. The latter condition is limited by the momentum relaxation of low-energy minority carriers in the base. If the ballistic scattering length is sufficiently long, then the speed of a coherent transistor is limited by the parasitics, as is evident from (34). This conclusion is borne out by the numerical analysis of an exemplary CT structure in the next section.

IV. Example

Let us discuss the possibility of a practical operation of the CT in an extended frequency range. The key condition underlying the above theory is collisionless transport of minority carriers across the base. Unfortunately, we are not aware of any reliable calculation of the scattering time for minority carriers in heavily doped semiconductors at low temperatures and, therefore, confine ourselves to simple estimates. Consider inelastic scattering processes first. Fulfillment of the inequality $\Delta < \hbar\omega_{\text{opt}}$ [cf. (2)] ensures that optical phonons cannot be emitted. Since we also need $kT << \Delta$ in order to suppress the Landau damping, it is clear that optical phonon scattering is not operative. Similar argument applies to inelastic scattering of minority carriers (electrons) by majority carriers (holes). For typical hole concentrations $p \gtrsim 10^{19}$ cm^{-3}, the plasmon energy is $\hbar\omega_p \gtrsim 50$ meV. Since in our case the electron kinetic energy is well below $\hbar\omega_p$, the inelastic interaction with holes is negligible.

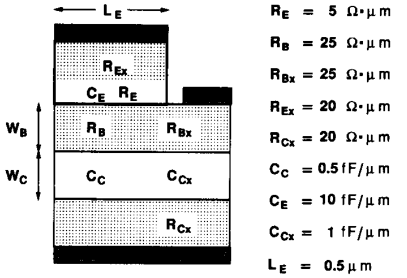

Fig. 7. Schematic diagram of an exemplary n-p-n heterostructure transistor and the parameters assumed per micrometer of the collector width into the page.

Elastic interaction of minority electrons with the screened Coulomb potential of impurities may be approximately described by the Brooks–Herring approach. A weakness of such estimates is in accounting for the screening by the degenerate hold gas, which is a "poor metal." Even at highest acceptor concentrations N_A, the Fermi–Thomas screening length r_0 is much shorter than $N_A^{-1/3}$. The strong screening effect ensures the validity of Born's approximation for the scattering of electrons. Thus calculated scattering cross section σ is practically independent of energy and scales as $\sigma \propto N_A^{1/3}$. Assuming that the base is made of GaAs with $N_A \approx 10^{19}$ cm^{-3}, we find $\sigma \approx 3 \times 10^{-15}$ cm^{-2}, whence the ballistic mean free path of minority electrons is about 2500 Å. Reliable data, either experimental or theoretical, for the ballistic times of flight of minority carriers in heavily doped semiconductor layers at low temperatures would be very valuable.

Fig. 7 shows the assumed parameters of the structure and estimated elements of the equivalent circuit, Fig. 5. We assume that the transistor is operated at 4.2 K, and that the ratio $\Delta/kT \equiv \tilde{\Delta} \approx 25$. The fact that $\tilde{\Delta}$ is so large is not important: coherent operation can be achieved with $\tilde{\Delta} \approx 5$ and even lower. Not specializing to a concrete heterostructure, we assume that the ballistic velocity in the base and the saturation velocity in the junction are equal and $\tau_B = \tau_C = 1$ ps.

The unilateral gain $|U|$ and the current gain $|h_{21}^e|^2$ of our exemplary circuit are plotted in Fig. 8. We see that the conventional f_T of this device would be about 100 GHz, but the transistor is active up to frequencies which are a factor of 2π higher. Interestingly, the current gain has been largely damped away by the parasitics, although a trace of the peak is clearly seen near $\omega\tau_S = 2\pi$.

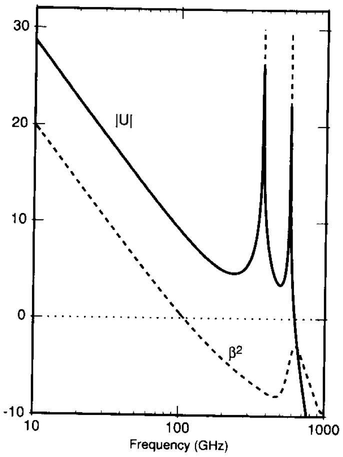

Fig. 8. The unilateral gain $|U|$ and the current gain $\beta \equiv |h_{21}^e|$ of an abrupt-junction ballistic transistor with the parameters as in Fig. 7.

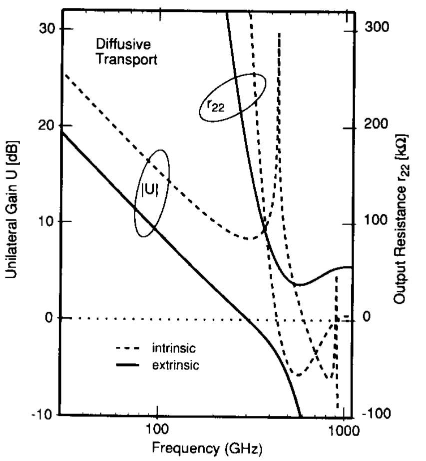

Fig. 10. The unilateral gain $|U|$ and the output resistance $r_{22} \equiv \text{Re}\,(z_{22}^e)$ of a diffusive transistor with the parameters as in Fig. 7.

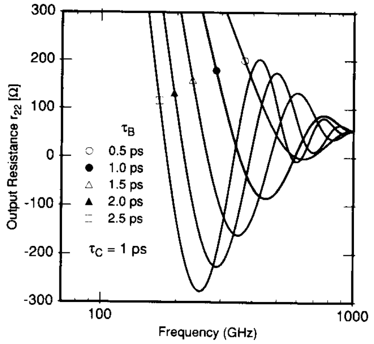

Fig. 9. Negative output resistance $r_{22} = \text{Re}\,(z_{22}^e)$ of an abrupt-junction ballistic transistor with the parameters as in Fig. 7, except the heterojunction spike Δ, which is varied so as to produce a desired $\tau_B = W_B(m/2\Delta)^{1/2}$.

Again, as in the intrinsic case, the unilateral gain is negative between the two peaks, indicating that Re $(z_{22}^e) < 0$ in that region. The output resistance is plotted in Fig. 9 for several values of the base transit time τ_B, which can be varied by changing Δ while keeping all other parameters as in Fig. 7. The $\tau_B = 1$ ps curve, corresponding to the case displayed in Fig. 8, is emphasized by a fatter line. We see that increasing τ_B shifts the onset of $r_{22} < 0$ to lower frequencies and enhances the magnitude of negative r_{22}. Thus for $\tau_B = 2$ ps, the $r_{22} < 0$ range occurs between 200 and 400 GHz with the center of activity near 300 GHz. In this case the tolerance of the parasitic elements would be considerably relaxed.

Let us compare the results in Figs. 8 and 9 against analogous calculations for a *diffusive* transistor with similar specifications. We have assumed an abrupt-junction HBT with the parameters identical to those in Fig. 7. The base transit time $\tau_D = W_B^2/2D = 1$ ps is adjusted by choosing a diffusion coefficient $D = 50$ cm^2/s. Fig. 10 shows the unilateral gain U and the output resistance r_{22}, calculated both in the intrinsic limit and including the parasitic elements. For simplicity, we have neglected the Early effect[4] and used (A.13)–(A.16) of the Appendix. We see that while the intrinsic U exhibits transit-time resonances, these effects are completely swamped by the device parasitics. The output resistance becomes negative only in the intrinsic case. This example confirms the result first obtained by Tiwari [8] and demonstrates the advantage of a coherent base propagation.

V. Conclusions

We have presented a theory of high-frequency behavior of abrupt-junction heterostructure bipolar transistors with a collisionless transport of minority carriers in the base.

Special "coherent" effects arise in the regime when the injected carriers form a collimated and monoenergetic beam in the base, i.e., in the limit when their average ballistic velocity is sufficiently large compared to the thermal spread in the velocity normal component. Realization of a coherent transistor is restricted to cryogenic temperatures.

Coherent base propagation results in the existence of resonances in the common-emitter current gain h_{21}^e at frequencies far exceeding the usual f_T of an intrinsic transistor. Moreover, they open up one or several wide bands of frequencies above f_T, where the transistor is active.

Characteristics of the coherent transistor have been further analyzed in an equivalent-circuit model in which the three terminals of an intrinsic device are loaded with parasitic resistances and capacitances. To facilitate the analysis, we have derived analytic expressions for U, h_{21}^e, and z_{22}^e which can be applied to heterojunction transistors both in the ballistic and the diffusion regimes. With the value of parasitic elements estimated from the standard low-temperature material parameters of an exemplary het-

---

[4] By using the general formulas given in the Appendix, we have verified that inclusion of the Early effect (with $V_A \gtrsim 500$ V) produces no tangible modification of the curves in Fig. 10 even at room temperature.

erostructure, we have found that the coherent transistor retains its active behavior in an extended frequency range.

Physically, the active behavior of a coherent transistor results from the phase shift between the collector current and voltage, acquired during the minority-carrier transit across the base. We have compared this effect with an analogous effect, discussed previously [3]–[8], in which a negative dynamic output resistance is achieved due to a phase shift in the carrier transit with a saturated velocity across the base–collector junction. For transistors with a diffusive base propagation, we share the pessimistic conclusion [8] that because of the practical limitation imposed by device parasitics, collector transit-time effects can hardly be used to extend the transistor activity to higher frequencies.

APPENDIX
EXPLICIT FORMULAS FOR SMALL-SIGNAL TRANSISTOR PARAMETERS

It is convenient to have explicit expressions for the quantities U, h_{21}^{e}, and z_{22}^{e} in terms of the parameters of the equivalent circuit in Fig. 5, with the two-port block surrounded by the dashed line represented by general common-base admittance parameters

$$Y^{bi} = \begin{bmatrix} y_{11} & y_{12} \\ y_{21} & y_{22} \end{bmatrix}. \tag{A1}$$

This block corresponds to an intrinsic transistor but excludes the base resistance R_B. Inclusion of the elements R_B and C_{Cx} leads to the following matrix:

$$\tilde{Y}^{b} = \begin{pmatrix} \tilde{y}_{11} & \tilde{y}_{12} \\ \tilde{y}_{21} & \tilde{y}_{22} \end{pmatrix} = \frac{1}{q}\begin{pmatrix} y_{11} + R_B\Delta_y & y_{12} - R_B\Delta_y \\ y_{21} - R_B\Delta_y & y_{22} + R_B\Delta_y + i\omega C_{Cx}q \end{pmatrix} \tag{A2}$$

where

$$q \equiv 1 + R_B\Sigma_y \tag{A3}$$

$$\Sigma_y \equiv y_{11} + y_{12} + y_{21} + y_{22} \tag{A4}$$

$$\Delta_y \equiv y_{11}y_{22} - y_{12}y_{21}. \tag{A5}$$

Inclusion of the remaining extrinsic elements in Fig. 5, viz. R_{Bx}, R_{Ex}, and R_{Cx}, yields

$$Y^{b} = \frac{1}{Q}\begin{pmatrix} y_{11} + R_B\Delta_y + (R_{Bx} + R_{Cx})\Delta_0 & y_{12} - R_B\Delta_y - R_{Bx}\Delta_0 \\ y_{21} - R_B\Delta_y - R_{Bx}\Delta_0 & y_{22} + R_B\Delta_y + (R_{Bx} + R_{Ex})\Delta_0 + iq\omega C_{Cx} \end{pmatrix} \tag{A6}$$

where

$$\begin{aligned} Q \equiv{}& 1 + y_{11}(R_B + R_{Bx} + R_{Ex}) + y_{22}(R_B + R_{Bx} + R_{Cx}) + (y_{12} + y_{21})(R_B + R_{Bx}) + \Delta_y R_B(R_{Cx} + R_{Ex}) \\ &+ iq\omega C_{Cx}(R_{Bx} + R_{Cx}) + \Delta_0(R_{Ex}R_{Cx} + R_{Ex}R_{Bx} + R_{Bx}R_{Cx}) \end{aligned} \tag{A7}$$

$$\Delta_0 \equiv \Delta_y(1 + i\omega C_{Cx}R_B) + i\omega C_{Cx}y_{11}. \tag{A8}$$

Matrix Y^b is the common-base admittance matrix of the full circuit in Fig. 5. The common-base impedance matrix of the full circuit is given by

$$Z^{b} = \begin{pmatrix} \dfrac{y_{22} + R_B\Delta_y + i\omega C_{Cx}q}{\Delta_0} + R_{Bx} + R_{Ex} & -\dfrac{y_{12} - R_B\Delta_y}{\Delta_0} + R_{Bx} \\ -\dfrac{y_{21} - R_B\Delta_y}{\Delta_0} + R_{Bx} & \dfrac{y_{11} + R_B\Delta_y}{\Delta_0} + R_{Bx} + R_{Cx} \end{pmatrix}. \tag{A9}$$

The common-emitter admittance and impedance matrices are of the form

$$Y^{b} = \frac{1}{Q}\begin{pmatrix} \Sigma_y + (R_{Ex} + R_{Cx})\Delta_0 + i\omega C_{Cx}q & -y_{12} - y_{22} - R_{Ex}\Delta_0 - i\omega C_{Cx}q \\ -y_{21} - y_{22} - R_{Ex}\Delta_0 - i\omega C_{Cx}q & y_{22} + (R_{Bx} + R_{Ex})\Delta_0 + R_B\Delta_y + i\omega C_{Cx}q \end{pmatrix} \tag{A10}$$

$$Z^{e} = \begin{pmatrix} \dfrac{y_{22} + R_B\Delta_y + i\omega C_{Cx}q}{\Delta_0} + R_{Bx} + R_{Ex} & \dfrac{y_{12} + y_{22} + i\omega C_{Cx}q}{\Delta_0} + R_{Ex} \\ \dfrac{y_{21} + y_{22} + i\omega C_{Cx}q}{\Delta_0} + R_{Ex} & \dfrac{\Sigma_y + i\omega C_{Cx}q}{\Delta_0} + R_{Ex} + R_{Cx} \end{pmatrix}. \tag{A11}$$

The common-emitter current gain can be expressed as follows:

$$h_{21}^{e} = \frac{y_{21}^{e}}{y_{11}^{e}}$$

$$= \frac{y_{11} + y_{12} + \Delta_0 R_{Cx}}{\Sigma_y(1 + i\omega C_{Cx} R_B) + q(R_{Ex} + R_{Cx}) + i\omega C_{Cx}} - 1. \tag{A12}$$

Since U is independent of the common lead configuration, it can be calculated using either (A9) or (A11) in (23a) [alternatively, using (A6) or (A10) in (23b)]. It is convenient to use (23a) and the common-base impedance parameters (A9). The general expression is very messy, but it simplifies considerably when the Early effect is absent. In this case, taking $y_{12} = 0$ and $y_{22} = i\omega C_C$ as elements of Y^{bi} in (A1) [cf. (21) or (22) with $g_A = 0$], we find for U the following expression:

$$U = \frac{|y_{21}|^2}{\mathrm{Re}\,(A_1 + A_2 + A_3)} \tag{A13}$$

where

$$\begin{aligned} A_1 = {} & y_{11} y_{21}^{*} (\omega^2 R_B C_{Cx} [R_{Bx} C_{Cx} + R_{Cx}(C_C + C_{Cx})] \\ & + i\omega [R_{Bx}(C_C + C_{Cx}) + (\omega R_B C_{Cx})^2 \\ & \cdot (R_{Bx} + R_{Cx}) C_C + R_B C_C]) \end{aligned} \tag{A14}$$

$$\begin{aligned} A_2 = {} & y_{11} \omega^2 ((R_{Bx} + R_{Cx}) [(C_C + C_{\mathrm{c}} \\ & + C_C^2 (\omega C_{Cx} R_B)^2] + R_B C_C^2) \end{aligned} \tag{A15}$$

$$\begin{aligned} A_3 = {} & |y_{11}|^2 \omega^2 (R_B [R_{Bx} C_{Cx}^2 + R_{Cx}(C_C + C_{Cx})^2 + R_{Ex} C_C^2] \\ & + (R_{Bx} R_{Ex} + R_{Bx} R_{Cx} + R_{Cx} R_{Ex}) \\ & \cdot [(C_C + C_{Cx})^2 + \omega^2 R_B^2 C_C C_{Cx}]). \end{aligned} \tag{A16}$$

Using the explicit form of y_{11} and y_{21} for a-HBT, viz. $y_{11} = g_E + i\omega C_E$ and $y_{21} = -g_E \alpha_B \alpha_C$, (A13)–(A16) reduce to (26), (27) in the text.

REFERENCES

[1] A. A. Grinberg and S. Luryi, "Ballistic versus diffusive base transport in the high-frequency characteristics of bipolar transistors," *Appl. Phys. Lett.*, vol. 60, pp. 2770–2772, 1992.

[2] H. Kroemer, "Heterostructure bipolar transistors and integrated circuits," *Proc. IEEE*, vol. 70, pp. 13–25, 1982.

[3] G. T. Wright, "Transistor transit-time oscillator," *Electron. Lett.*, vol. 3, pp. 234–235, 1967.

[4] G. T. Wright, "Small-signal theory of the transistor transit-time oscillator (translator)," *Solid-State Electron.*, vol. 22, pp. 399–403, 1979.

[5] Y. Druelle, Y. Crosnier, and G. Salmer, "Large-signal behavior and capability of the transistor transit-time oscillator," *Proc. Inst. Elec. Eng.*, vol. 127, pt. 1, pp. 72–77, 1980.

[6] N. Dagli, W. Lee, S. Prasad, and C. G. Fonstad, "High-frequency characteristics of inverted-mode heterojunction bipolar transistors," *IEEE Electron Device Lett.*, vol. EDL-8, pp. 472–474, 1987.

[7] N. Dagli, "Physical origin of the negative output resistance of heterojunction bipolar transistors," *IEEE Electron Device Lett.*, vol. 9, pp. 113–115, 1988.

[8] S. Tiwari, "Frequency dependence of the unilateral gain in bipolar transistors," *IEEE Electron Device Lett.*, vol. 10, pp. 574–576, 1989.

[9] N. Dagli, "A unipolar transistor with negative output resistance," *Solid-State Electron.*, vol. 33, pp. 831–836, 1990.

[10] P. Roblin and S. C. Kang, "Unilateral power gain resonances and roll-off with frequency for the velocity-saturated MOSFET/MODFET wave equation," *IEEE Trans. Electron Devices*, vol. 39, pp. 1490–1495, 1992.

[11] S. M. Sze, *Physics of Semiconductor Devices.* New York: Wiley-Interscience, 1981, ch. 10.

[12] S. J. Mason, "Power gain in feedback amplifiers," *IRE Trans. Circuit Theory*, vol. CT-1, pp. 20–25, 1954.

[13] W. Shockley, *Electrons and Holes in Semiconductors.* Princeton, NJ: Van Nostrand, 1950, sec. 4.1c.

[14] N. G. van Kampen, *Stochastic Processes in Physics and Chemistry.* Amsterdam, The Netherlands: North Holland, 1981, sect. 1.6.

[15] W. Shockley, "Currents to conductors induced by a moving point charge," *J. Appl. Phys.*, vol. 9, pp. 635–636, 1938.

[16] A. A. Grinberg and S. Luryi, "Dynamic Early effect in heterojunction bipolar transistors," *IEEE Electron Device Lett.*, vol. 14, pp. 292–294, 1993.

[17] A. A. Grinberg and S. Luryi, "On the thermionic-diffusion theory of minority transport in heterostructure bipolar transistors," *IEEE Trans. Electron Devices*, vol. 40, pp. 859–866, May 1993.

[18] R. L. Pritchard, *Electrical Characteristics of Transistors.* New York: McGraw-Hill, 1967.

[19] S. Tiwari, *Compound Semiconductor Device Physics.* San Diego: Academic Press, 1992, ch. 7.

Anatoly A. Grinberg, photograph and biography not available at the time of publication.

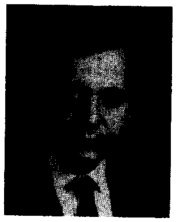

Serge Luryi (M'81–SM'85–F'90) received the Ph.D. degree in physics from the University of Toronto, Toronto, Ont., Canada, in 1978.

In 1980, he has been with AT&T Bell Laboratories, Murray Hill, NJ, where he is currently a Distinguished Member of Technical Staff in the Optoelectronic Device Research Department. His main research interests are in the physics of exploratory semiconductor devices.

During 1986–1990, Dr. Luryi was the Editor of IEEE TRANSACTIONS ON ELECTRON DEVICES.